Aggregation Induced Phosphorescent *N*-Oxyde-2,2'-Bipyridine Bismuth Complexes and Polymorphism-Dependent Emission.

Oksana Toma,[†] Nicolas Mercier,*[†] Magali Allain,[†] Alessandra Forni,*[γ] Franco Meinardi[‡] and Chiara Botta*[§]

Supporting Information

A- Synthesis

a) *bp2mo*, N-oxide-2,2'-bipyridinium
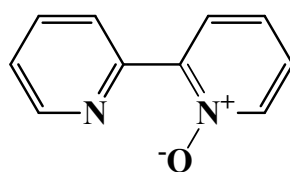
M = 172,18 g/mol

According to the literature[1], to a solution of 2,2'-bipyridine (7.0 g, 45mmol) in CH_2Cl_2 (50 ml) is added dropwise a solution of 3-chloroperbenzoic acid (mCPBA) (10.0 g, 58 mmol) in CH_2Cl_2 (80 ml) at 5-10°C. The reaction mixture is stirred at room temperature overnight. 2 M NaOH (100 mL) was added at 0°C and the mixture is stirred for 15 min. The organic layer is separated and washed with 2M NaOH (100 mL) once more. The combined basic washings are extracted with CH_2Cl_2 (3 x 100 mL). The CH_2Cl_2 phase is dried over solid Na_2CO_3 and evaporated to give N-oxide-2,2'-bipyridine (bp2mo). Recrystallization from ether/hexanes of the sample give white – beige crystals (5.6 g, 72 %).

RMN ¹H (300 MHz, $CDCl_3$, ppm): δ=8,89 (dd, 1H, J=6,9 Hz, H-3), 8,72 (ddd, 1H, J=6,2 Hz, H-6), 8,32 (dd, 1H, J=6,1 Hz, H-6'), 8,17 (dd, 1H, J=6,1 Hz, H-3'), 7,83 (ddd, 1H, J=6,3 Hz, H-4), 7,39-7,24 (m, 3H, H-4', H-5, H-5').

[¹] Norrby, T.; Borje, A.; Zhang, L.; Akermark, B. *Acta Chem Scand* **1998**, 52, 77.

b) __Materials__

All three phases α-(**1**), β-(**2**), γ-[BiBr₃(*bp2mo*)₂] (**3**) were synthetized by solvotermal method from the mixture of $BiBr_3$ and *bp2mo* with acetonitrile as solvent; for (**1**), 1 eq. of $BiBr_3$ and 2 eq. of *bp2mo*, heating for 13 h from 25 to 70°C, then kept for 30 h at 70°C, followed by a cooling down to 25°C during 18 h; for (**2**), 1 eq. of $BiBr_3$ and 4 eq. of *bp2mo*, heating for 3 h from 25 to 75°C, then kept at 75°C for 8 h, followed by a cooling down to 25°C during 4 h; for (**3**), 1 eq. of $BiBr_3$ and 2 eq. of *bp2mo*, heating for 3 h from 25 to 105°C, then kept at 105°C for 8 h, followed by a cooling down to 25°C during 4 h. The solvent of the obtained yellow solutions was further evaporated to give yellow needle – like crystals of (1), yellow block – like crystals of (2) and yellow plate – like crystals of (3), which were filtered off and washed with acetonitrile. The phase purity of all compounds was checked by XRPD diffraction method using a D8 Bruker diffractometer (Cu-K$\alpha_{1,2}$ radiation) equipped with a linear Vantec super speed detector (S.I.).

__Elemental analyses__:
α phase: element(theoretical%/experimental%): C (30.28/30.15); N (7.06/7.01); H (2.02/1.99)
β phase: element(theoretical%/experimental%): C (30.28/30.17); N (7.06/6.97); H (2.02/1.98)
γ phase: element(theoretical%/experimental%): C (30.28/30.31); N (7.06/7.00); H (2.02/2.03)

B-Single Crystal data

X-ray diffraction data were collected at T= 293 K on a Bruker-Nonius KAPPA-CDD with MoKα radiation (λ=0.71073Å) (**2**) or a Agilent Supernova with CuKα radiation (λ=1.5407Å) diffractometers (**1**, **3**).

__B1- α-[BiBr₃(*bp2mo*)₂] (1)__ Summary of crystallographic data

Empirical formula	C20 H16 Bi Br3 N4 O2
Formula weight	793.08
Temperature	293.0(1) K
Wavelength	1.54184 A
Crystal system, space group	Triclinic, P -1
Unit cell dimensions	a = 9.6004(4) A alpha = 97.53(1) deg.
	b = 15.6899(4) A beta = 93.73(1) deg.
	c = 22.9678(5) A gamma = 96.04(1) deg.
Volume	3399.76(18) A^3
Z, Calculated density	6, 2.324 Mg/m^3
Absorption coefficient	21.674 mm^-1

F(000)   2208

Crystal size   0.11 x 0.06 x 0.05 mm

Theta range for data collection   2.86 to 76.78 deg.

Limiting indices   -12<=h<=11, -19<=k<=19, -26<=l<=28

Reflections collected / unique   35956 / 13883 [R(int) = 0.0347]

Completeness to theta = 76.78   97.1 %

Absorption correction   Semi-empirical from equivalents

Max. and min. transmission   1.00000 and 0.61430

Refinement method   Full-matrix least-squares on F^2

Data / restraints / parameters   13883 / 0 / 811

Goodness-of-fit on F^2   1.171

Final R indices [I>2sigma(I)]   R1 = 0.0286, wR2 = 0.0700

R indices (all data)   R1 = 0.0384, wR2 = 0.0995

Largest diff. peak and hole   1.129 and -1.439 e.A^-3
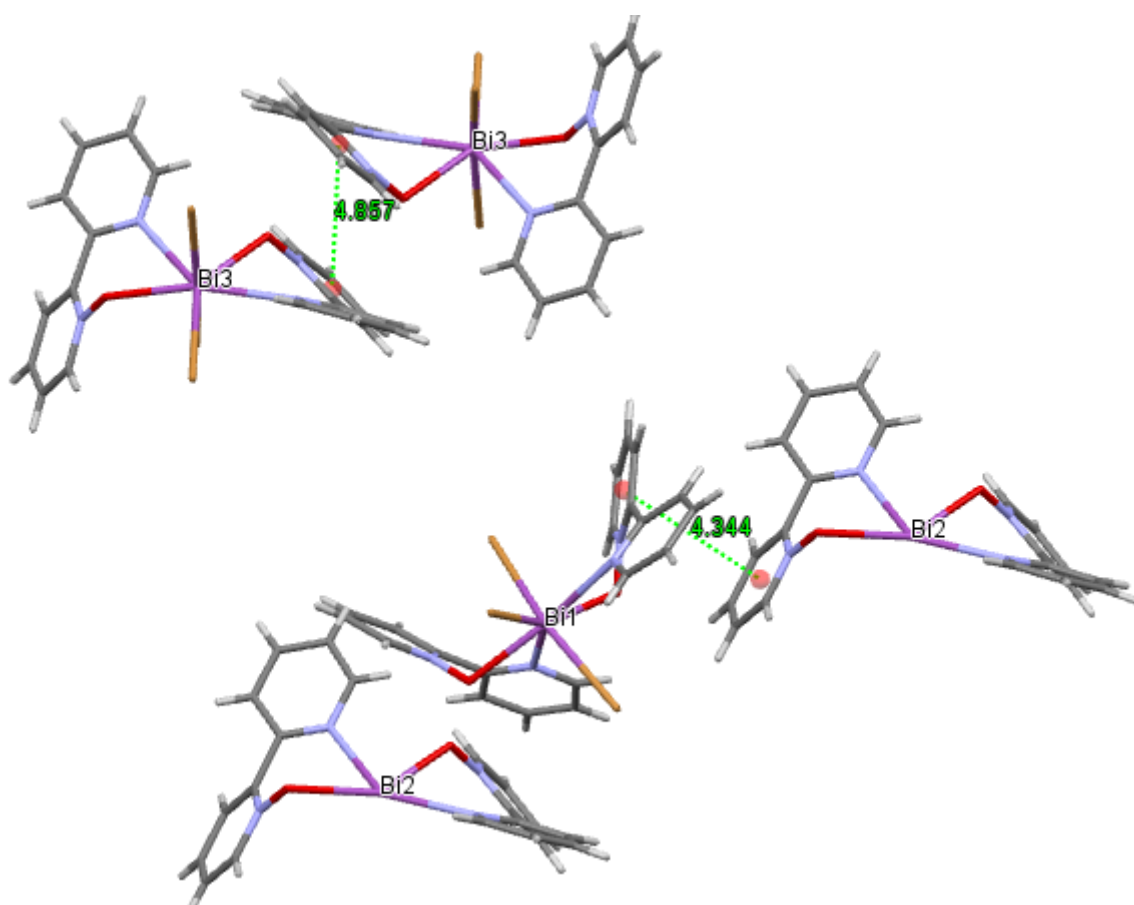
Fig. S1. Crystal packing of **1** evidencing the weak π-π interactions present in the structure and the distances between the centroids of the involved rings.

B2- δ-[BiBr₃(*bp2mo*)₂] *(2)* Summary of crystallographic data

Empirical formula	C20 H16 Bi Br3 N4 O2
Formula weight	793.08
Temperature	293(2) K
Wavelength	0.71073 A
Crystal system, space group	Monoclinic, P 1 21/n 1
Unit cell dimensions	a = 9.748(1) A, alpha = 90 deg.
	b = 13.011(1) A, beta = 91.88(1) deg.
	c = 18.253(3) A, gamma = 90 deg.
Volume	2313.8(5) A^3
Z, Calculated density	4, 2.277 Mg/m^3
Absorption coefficient	12.824 mm^-1
F(000)	1472
Crystal size	0.11 x 0.06 x 0.06 mm
Theta range for data collection	2.23 to 28.59 deg.
Limiting indices	-13<=h<=13, -17<=k<=17, -24<=l<=24
Reflections collected / unique	25911 / 5867 [R(int) = 0.1073]
Completeness to theta = 28.59	99.1 %
Absorption correction	Semi-empirical from equivalents
Max. and min. transmission	0.463 and 0.2997
Refinement method	Full-matrix least-squares on F^2
Data / restraints / parameters	5867 / 0 / 271
Goodness-of-fit on F^2	1.020
Final R indices [I>2sigma(I)]	R1 = 0.0716, wR2 = 0.1825
R indices (all data)	R1 = 0.1497, wR2 = 0.2454
Largest diff. peak and hole	1.403 and -3.684 e.A^-3
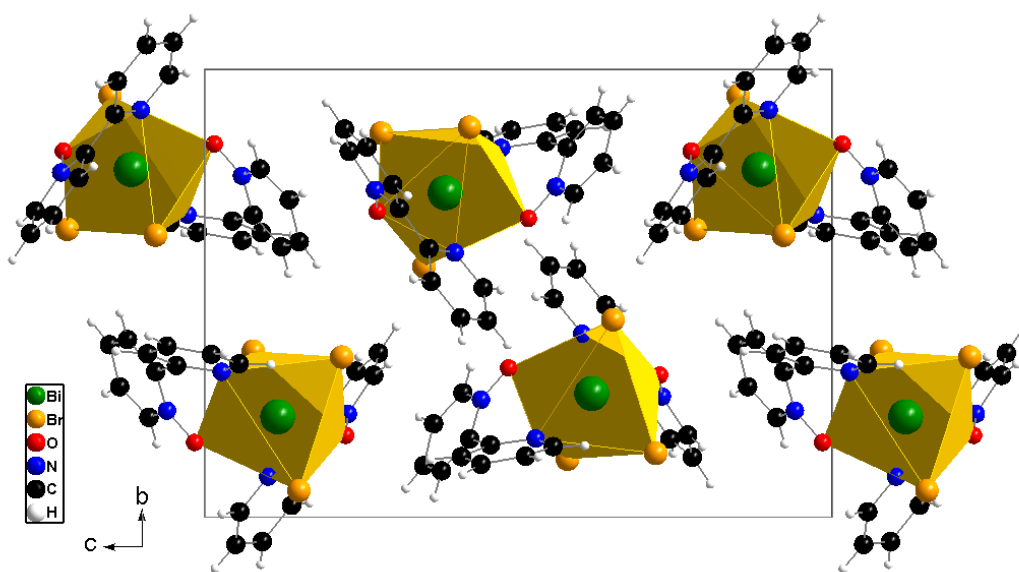
Fig. S2. General view along a of the structure of β-[BiBr$_3$(*bp2mo*)$_2$]

B3- γ-[BiBr₃(*bp2mo*)₂] *(3)* Summary of crystallographic data

Empirical formula   C20 H16 Bi Br3 N4 O2

Formula weight   793.08

Temperature   293.0(1) K

Wavelength   1.54184 A

Crystal system, space group   Monoclinic, P 1 21/c 1

Unit cell dimensions   a = 13.5654(1) A   alpha = 90 deg.

b = 9.6701(1) A   beta = 94.96(1) deg.

c = 18.1116(2) A   gamma = 90 deg.

Volume   2366.97(4) A^3

Z, Calculated density   4, 2.226 Mg/m^3

Absorption coefficient   20.754 mm^-1

F(000)   1472

Crystal size   0.29 x 0.20 x 0.16 mm

Theta range for data collection   3.27 to 76.47 deg.

Limiting indices   -12<=h<=16, -12<=k<=11, -22<=l<=20

Reflections collected / unique   10686 / 4865 [R(int) = 0.0453]

Completeness to theta = 76.47   98.0 %

Absorption correction   Semi-empirical from equivalents

Max. and min. transmission   1.00000 and 0.22785

Refinement method   Full-matrix least-squares on F^2

Data / restraints / parameters   4865 / 0 / 271

Goodness-of-fit on F^2   1.084

Final R indices [I>2sigma(I)]   R1 = 0.0400, wR2 = 0.1044

R indices (all data)   R1 = 0.0466, wR2 = 0.1109

Largest diff. peak and hole   3.244 and -2.326 e.A^-3
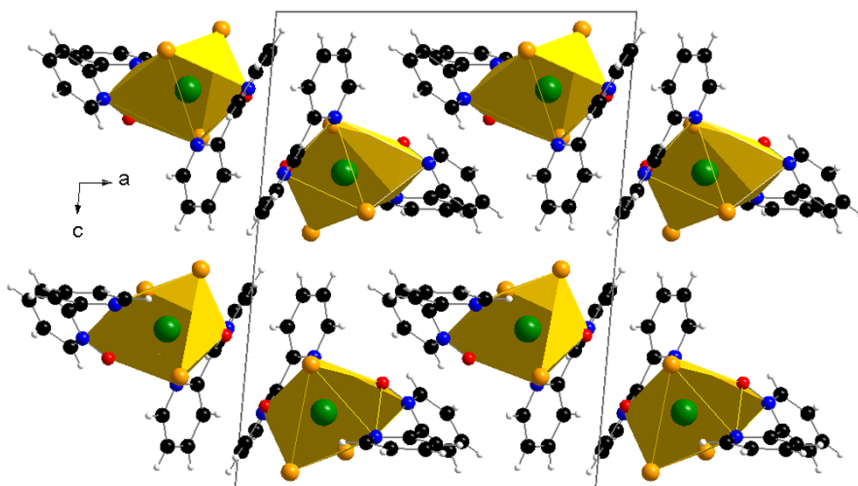
Fig. S3 – General view along b of the structure of γ-[BiBr$_3$($bp2mo$)$_2$]

C-XRPD (powder diffraction)

Powder X-Ray patterns of the homogenous samples of 1 – 3 showed that all reflections are indexed in the unit cells obtained from single crystal X-ray diffraction studies (see above).

C1- α-[BiBr$_3$($bp2mo$)$_2$] (1)
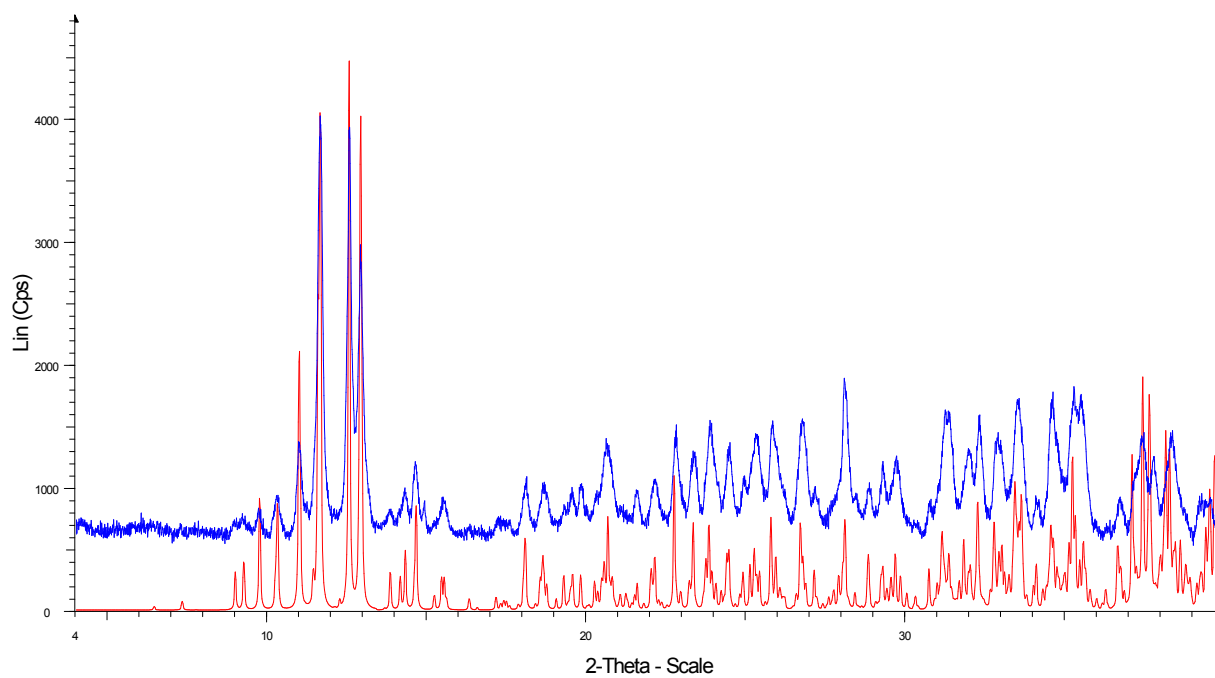
Fig. S4 – Experimental (blue) end calculated (red) XRPD of (1).

C2- β-[BiBr₃(*bp2mo*)₂] *(2)* Summary of crystallographic data
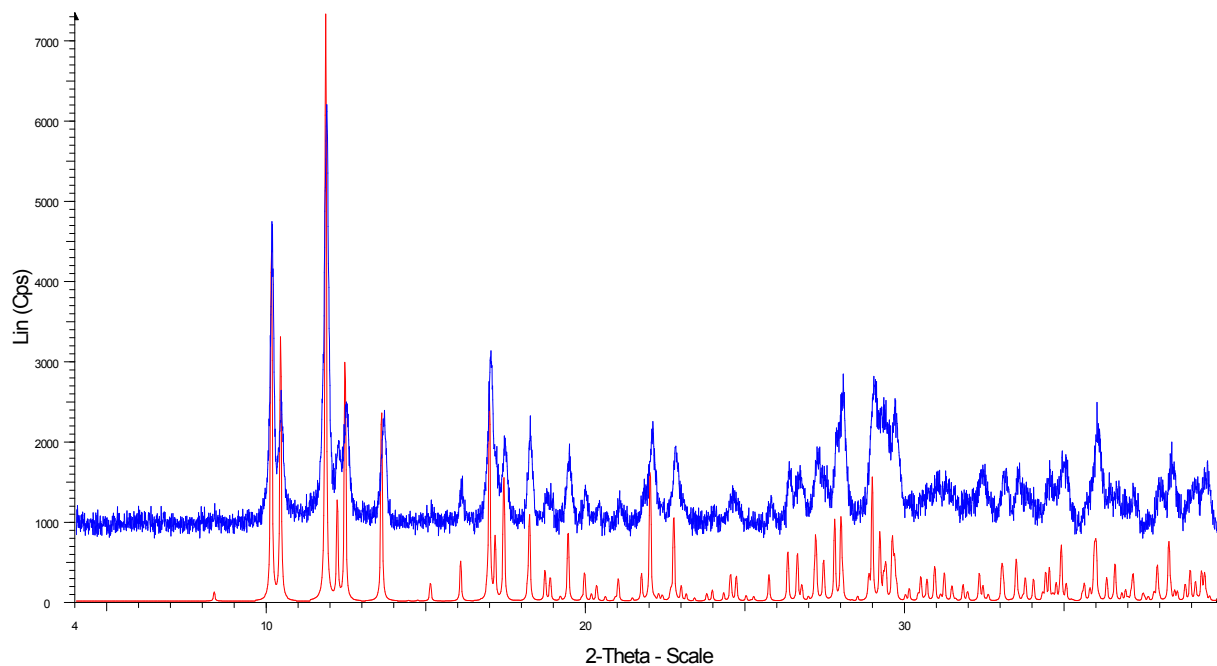
Fig. S5 – Experimental (blue) end calculated (red) XRPD of (2).

C3- γ-[BiBr₃(*bp2mo*)₂] *(3)* Summary of crystallographic data
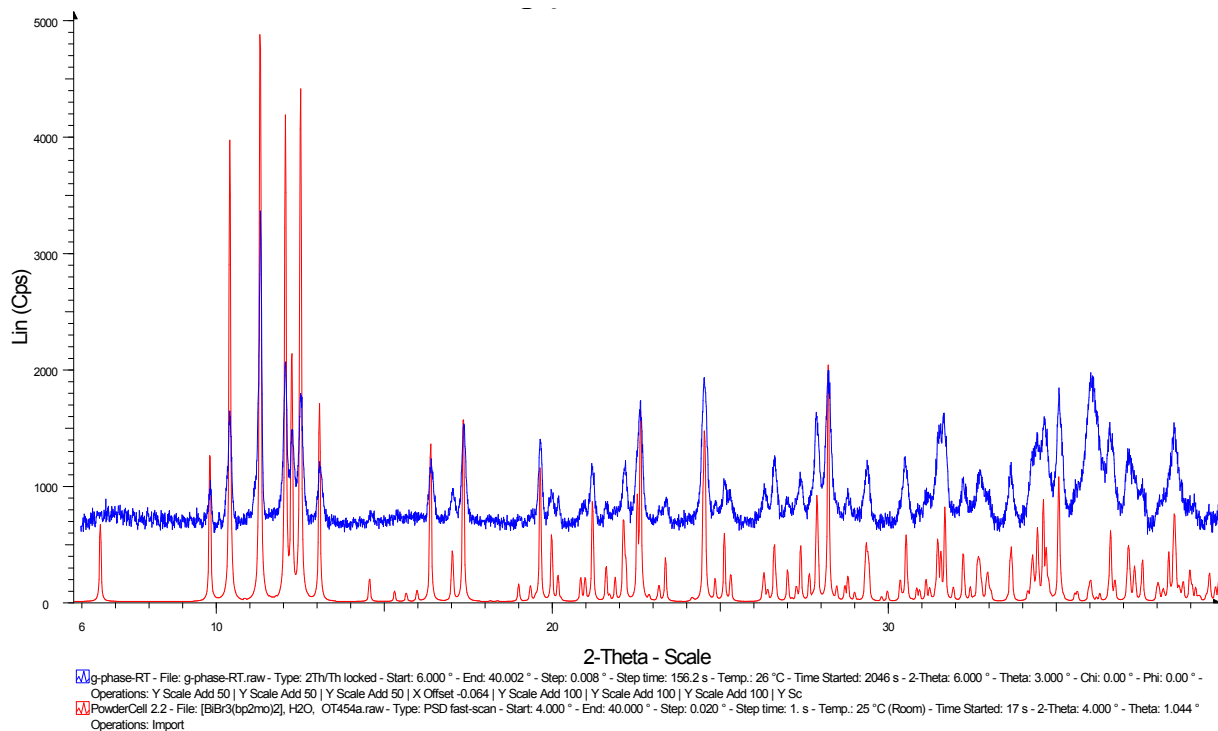
Fig. S6– Experimental (blue) end calculated (red) XRPD of (3).

D- Optical properties

UV-Vis optical absorption measurements are performed using a Perkin-Elmer Lambda-9 spectrometer on solutions and solid state KBr pellets. PL continuous wave (CW) measurements are obtained with a SPEX 270 M monochromator equipped with a N_2 cooled charge-coupled device exciting with a monochromated Xe lamp or an Ar^+ laser. The spectra are corrected for the instrument response. PL QY on solid state materials is obtained with a home-made integrating sphere by correcting for the background of the exciting lamp.[2]. Low temperature measurements have been obtained by using a two chamber Oxford LN_2 cryostat.

The time-resolved PL measurements involved two set-ups depending on the requested time resolution. For slow decaying PL emissions, samples were excited at a 405 nm (3.06 eV) using an Edimburgh EPL 405 pulsed laser diode, and the signal was detected in photon-counting mode using a Hamamatsu R943-02 photomultiplier connected to an Ortec 9353 multichannel scaler. The overall time resolution was better than 1 ns. In the case of sub ns signals the excitation source was the second harmonic of a Ti:Sapphire laser and the emission was analized with a Hamamatsu C5680 streak camera. In this case the system resolution was around 4 ps.
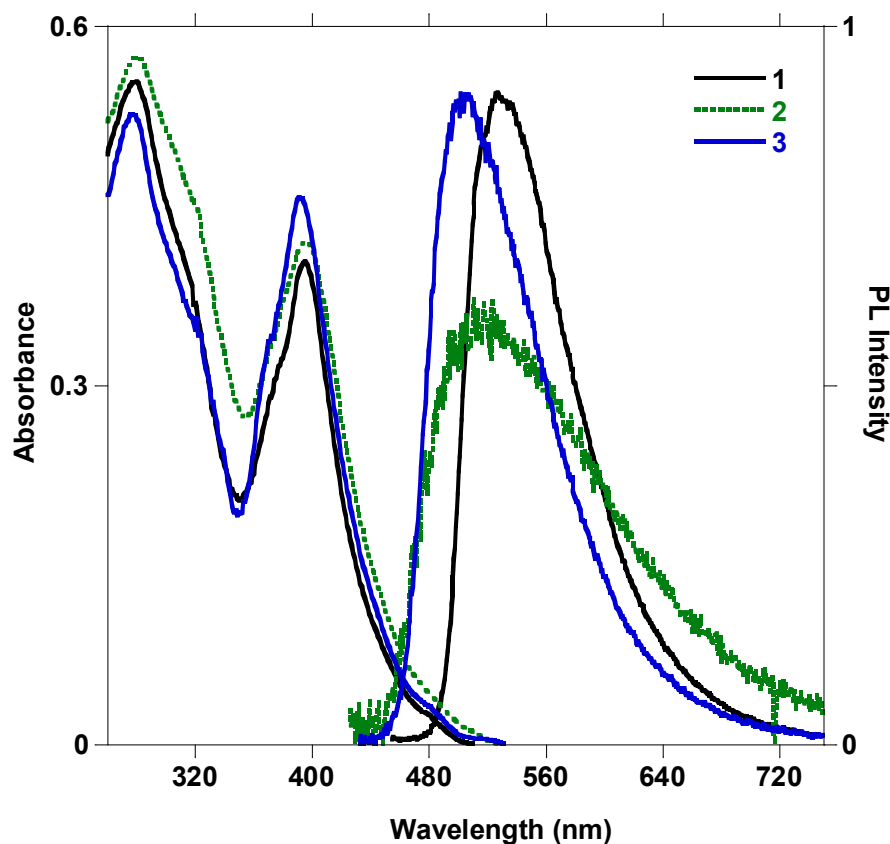
Fig. S7. Absorption and PL spectra of **1**, **2** and **3** in the solid state.
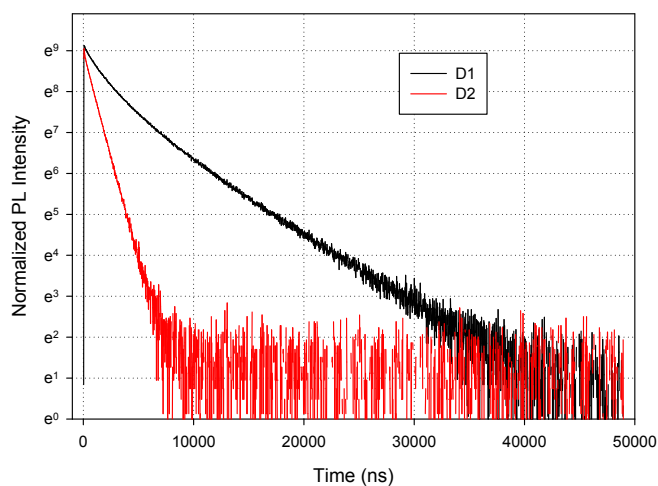
Fig. S8. PL decays of the solid state **1** (black) and **3** (red) complexes
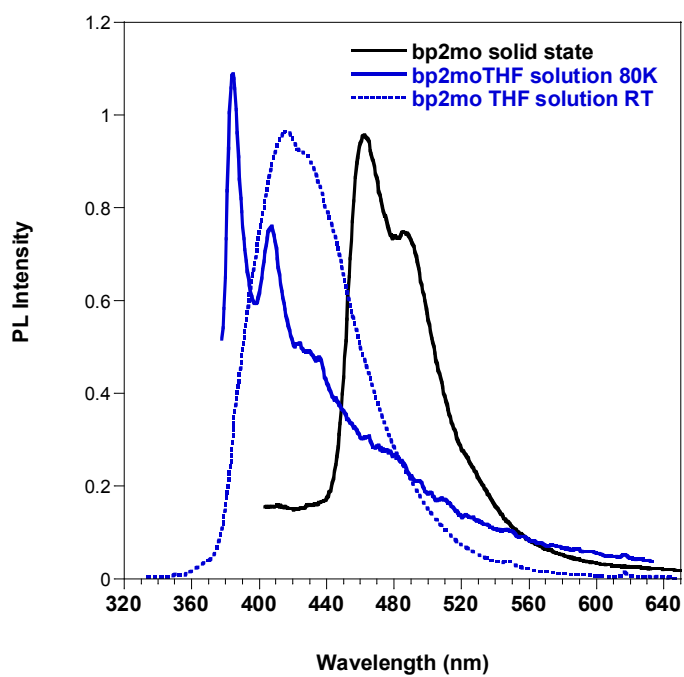
Fig. S9. Emission properties of *bp2mo* solutions in THF at room temperature and 80K, compared with the emission of the powder.
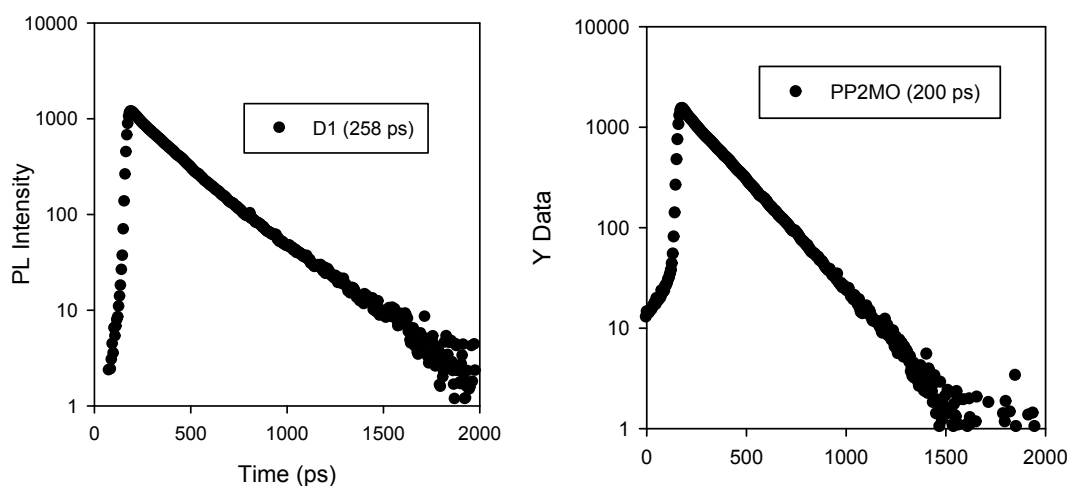
Fig. S10. PL decays of **1** (left) and *bp2mo* (right) in THF solutions

Table S1. Emission properties of BiBr$_3$(*bp2mo*)$_2$ (radiative and non-radiative parameters are obtained from the QY and lifetime experimental results)

	λ / nm	PL QY (%)	τ	k_R (s^{-1})	k_{NR} (s^{-1})
1 α crystal	528	17	4.8 μs	3.6x10^4	1.7x10^5
2 β crystal	515	0.5	NA		
3 γ crystal	502	5	1.0 μs	5.0x10^4	9.5x10^5
BiBr$_3$(*bp2mo*)$_2$ solution	442	0.01	258 ps		
bp2mo solution	415	<0.01	200 ps		

(2) J. Moreau, U. Giovanella, J-P. Bombenger, W. Porzio, V. Vohra, L. Spadacini, G. Di Silvestro, L. Barba, G. Arrighetti, S. Destri, M. Pasini, M. Saba, F. Quochi, A. Mura, G. Bongiovanni, M. Fiorini, M. Uslenghi, C. Botta, *ChemPhysChem*., **2009**, *10*, 647

E- Computational studies

Computational studies have been performed on the *bp2mo* ligand and the BiBr$_3$(*bp2mo*)$_2$ complex, using the Gaussian 09 suite of programs.[3] Starting from the experimental structure of **3**, the geometry of BiBr$_3$(*bp2mo*)$_2$ has been optimized *in vacuo* within the DFT approach using the M06 functional,[4] which was properly developed to treat organometallic systems. Other calculations have been performed on the X-ray crystal geometries of polymorphs **1-3**. All atoms have been described by the def2-SVP split valence basis set with polarization functions.[5] Bismuth has been treated as a 23-electron system, with relativistic effective core potentials (ECP's) taken from the literature.[6] Standard vertical Time Dependent (TD) DFT calculations[7] were carried out with the same basis set to determine the excited state properties at both the optimized and X-ray geometries. Among several tested functionals, i.e. M06, PBE0, CAM-B3LYP, ωB97X and M062X, the latter[4] showed the better agreement with the experimental absorption spectrum. 25 vertical singlet excitations from the ground state (S$_0$) have been evaluated. The lower energy singlet (S$_1$) excited state was then submitted to TD-M062X geometry optimization to evaluate the emission from S$_1$ to S$_0$. To determine the lowest energy triplet state of the complex (T$_1$), an unrestricted UM06/def2-SVP triplet optimization has been performed, starting from the optimized S$_0$ geometry of the complex. This represents an approximation to the real T$_1$ TDDFT minimum, which however in no way was located by means of the TDDFT optimization procedure. It is worth noting that TDDFT calculations do not provide information on oscillator strengths for triplet-singlet transitions since spin-orbit coupling effects are not included in current TDDFT implementations.

The structure of the ligand has been optimized *in vacuo* within the DFT approach using the same functional as used for the complex (M06). In place of the limited SVP basis set used for the complex, whose choice was imposed by the need of using a balanced basis set for all atoms, we used for the ligand a more accurate basis set, 6-311++G(d,p), which is not available for Bismuth. TDDFT calculations of the excited state properties have been performed with the PBE0 functional,[8] which in this case provided the better agreement with experiment.

[3] Frisch, M. J. et al. *Gaussian 09, Revision D.01.*, Gaussian, Inc.: Wallingford, CT, USA, **2013**.

[4] Zhao, Y.; Truhlar, D. *Theo. Chem. Accounts* **2008**, *120*, 215.

[5] F. Weigend and R. Ahlrichs, *Phys. Chem. Chem. Phys.* **2005**, *7*, 3297.

[6] B. Metz, H. Stoll, M. Dolg, J. Chem. Phys. **2000**, *113*, 2563.

[7] (a) E. Runge and E. K. U. Gross, *Phys. Rev. Lett.*, **1984**, *52*, 997; (b) R. E. Stratmann, G. E. Scuseria, M. J. Frisch, *J. Chem. Phys.*, **1998**, *109*, 8218; (c) M. E. Casida, *J. Mol. Struct. (THEOCHEM)* **2009**, *914*, 3.

[8] (a) M. Ernzerhof and G. E. Scuseria, *J. Chem. Phys.*, **1999**, *110*, 5029; (b) C. Adamo and V. Barone, *J. Chem. Phys.*, **1999**, *110,* 6158.

Table S2. TD-M062X/def2-SVP absorption wavelengths (nm) with associated oscillator strengths *f*, computed at the experimental geometry, for molecules **1a**, **1b**, **1c**, **2** and **3**.

	1a	1b	1c	2	3
λ_1 (*f*)[a]	419 (0.037)	414 (0.047)	407 (0.030)	449 (0.024)	420 (0.032)
λ_2 (*f*)[b]	395 (0.016)	395 (0.006)	387 (0.015)	390 (0.039)	387 (0.023)

[a] Major contribution: HOMO→LUMO; [b] Major contribution: HOMO→LUMO+1
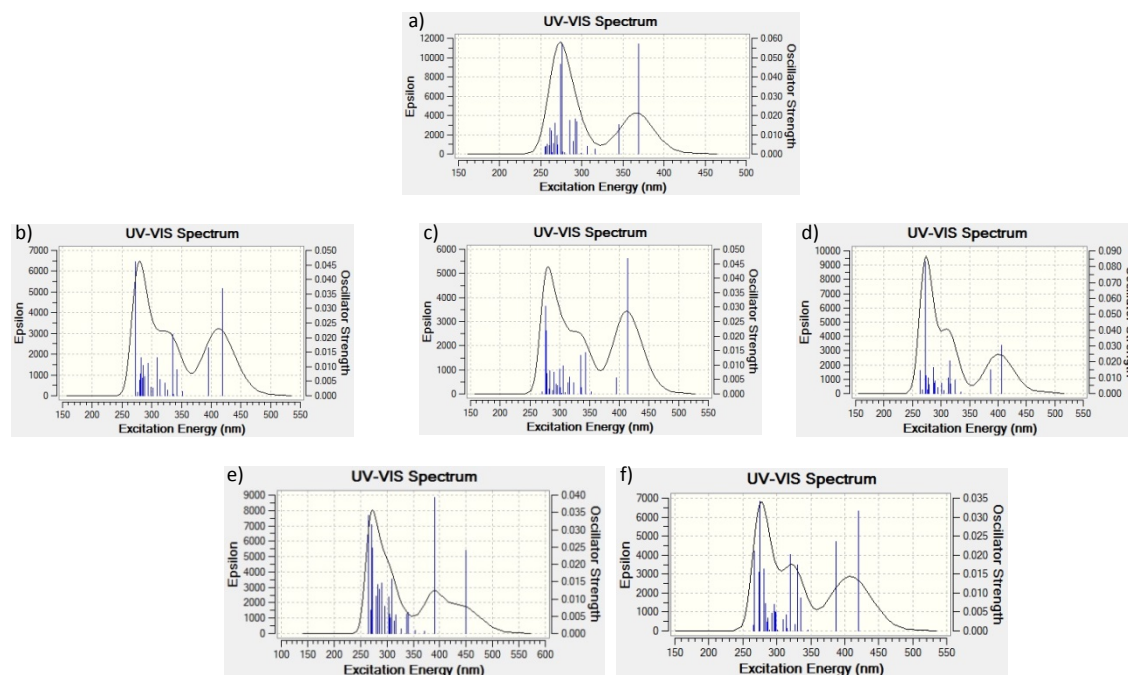
Fig. S11. TD-M062X/def2-SVP absorption spectra of [BiBr₃(*bp2mo*)₂] at the optimized geometry (a) and at the X-ray crystal geometries of **1a** (b), **1b** (c), **1c** (d), **2** (e) and **3** (f), obtained by convolution of the blue sticks with 0.2 eV of half-bandwidth.
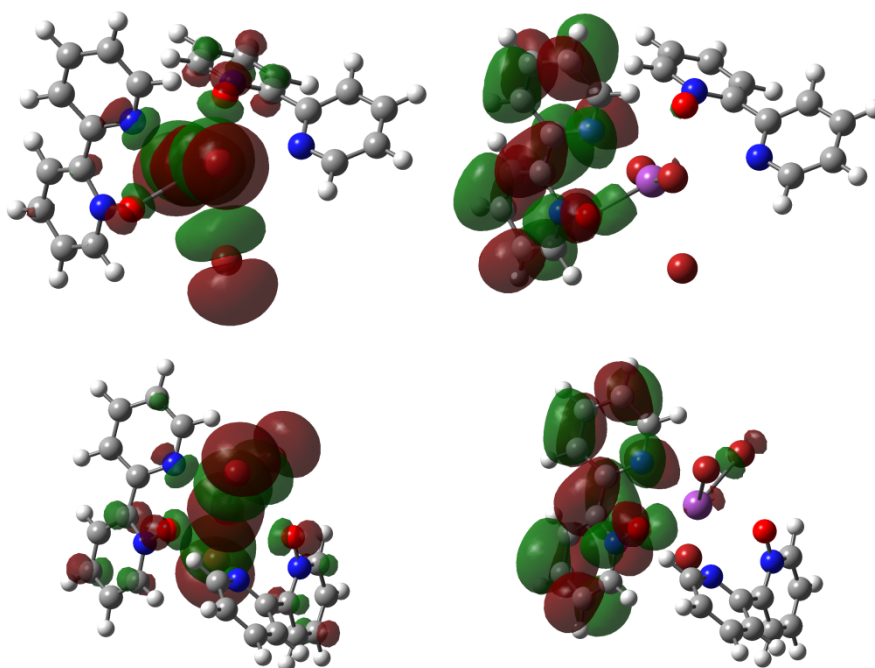
Fig. S12. Plots of the M062X/def2-SVP HOMO (left) and LUMO (right) of [BiBr$_3$(*bp2mo*)$_2$] at the optimized geometries of S1 (top) and T1 (bottom). For each plot, the more planar ligand is on the left and the less planar one is on the right. Isosurfaces value 0.02.

Table S3. Intermolecular hydrogen bonds shorter than the sum of the van der Waals radii in **1**-**3**.

	H⋯Y/Å	C–H⋯Y/°
1		
C–H⋯O		
C2–H2⋯O4	2.525	163
C51–H51⋯O6	2.360	133
C–H⋯Br		
C8–H8⋯Br1	2.997	127
C32–H32⋯Br2	2.980	145
C13–H13⋯Br3	3.004	144
C59–H59⋯Br4	3.003	158
C38–H38⋯Br6	3.040	133
C28–H28⋯Br7	2.918	126
C24–H24⋯Br8	3.038	136
C54–H54⋯Br8	2.924	138
C–H⋯π		
C58–H58⋯C32	2.820	132
C23–H23⋯C53	2.818	154
C50–H50⋯C57	2.882	138
2		
C–H⋯O		
C10–H10⋯O2	2.658	122
C17–H17⋯O1	2.692	146
C–H⋯Br		
C19–H19⋯Br1	3.029	173
C7–H7⋯Br2	3.011	140
C3–H3⋯Br3	2.987	149
C12–H12⋯Br3	3.000	136
C13–H13⋯Br3	2.967	129
C–H⋯π		
C1–H1⋯C8	2.853	155
C20–H20⋯C4	2.888	134
3		
C–H⋯O		
C2–H2⋯O1	2.515	149
C17–H17⋯O2	2.413	162
C–H⋯Br		
C11–H11⋯Br1	2.879	137
C9–H9⋯Br2	2.942	169
C19–H19⋯Br2	3.038	130
C14–H14⋯Br3	2.803	159
C–H⋯π		
C7–H7⋯C19	2.742	147

F- Photos of samples

-a-

-b-